

Synthesis and efficient field emission characteristics of patterned ZnO nanowires*

Zhang Yongai(张永爱), Wu Chaoxing(吴朝兴), Zheng Yong(郑泳), and Guo Tailiang(郭太良)[†]

College of Physics and Information Engineering, Fuzhou University, Fuzhou 350002, China

Abstract: Patterned ZnO nanowires were successfully synthesized on ITO electrodes deposited on the glass substrate by using a simple thermal evaporation approach. The morphology, crystallinity and optical properties of ZnO nanowires were characterized by scanning electron microscopy, X-ray diffraction, energy dispersive X-ray and photoluminescence spectroscopy. Their field emission characteristics were also investigated. SEM images showed that the ZnO nanowires, with a diameter of 100–200 nm and length up to 5 μm , were highly uniform and well distributed on the linear ITO electrodes. The field emission measurement indicated that patterned ZnO nanowire arrays have a turn-on field of 1.6 V/ μm at current density of 1 $\mu\text{A}/\text{cm}^2$ and a threshold field of 4.92 V/ μm at current density of 1 mA/ cm^2 at an emitter-anode gap of 700 μm . The current density rapidly reached 2.26 mA/ cm^2 at an applied field of 5.38 V/ μm . The fluctuation of emission current was lower than 5% for 4.5 h. The low turn-on field, high current density and good stability of patterned ZnO nanowire arrays indicate that it is a promising candidate for field emission application.

Key words: zinc oxide; nanowires; patterned growth; field emission

DOI: 10.1088/1674-4926/33/2/023001

PACC: 7840G; 6146; 8115H

1. Introduction

Field emission emitters, including carbon nanotubes (CNTs), SiC, Si and SnO₂ have been extensively investigated due to their high aspect ratio, small tip radius and low electron affinity in the past years^[1–4]. Among them, great attention has been paid to CNTs due to their low turn-on field strength and large emission current density. However, the advancement of field emission electron sources employing CNTs has been confronted with the drawbacks (such as the lack of long-term emission stability) those CNTs as field emission electron sources undergo, including an irreversible gradation under an oxygen atmosphere and a high temperature condition, which will limit their applications^[5, 6]. Due to a wide band-gap ($E_g = 3.37$ eV), large excitation binding energy (60 meV) at room temperature and high mechanical and thermal stabilities, zinc oxide (ZnO) possesses promising applications in ultraviolet lasers^[7], actuators^[8], sensors^[9] and field emission arrays^[10–13].

Up to now, numerous ZnO nanostructures such as nanoinjectors^[10], nanotube/nanorod^[14], nanobottles^[15] and nanowires^[11, 13] have been synthesized by thermal evaporation^[16–18], pulsed laser deposition^[19], hydrothermal decomposition^[20] and chemical vapour deposition^[21]. Their characteristics and potential applications have also been studied intensively. However, one key challenge is to develop efficient deposition technique to assemble a ZnO electron source and form patterned ZnO arrays. Lin *et al.*^[22] has reported a turn-on field of 2.5 V/ μm at a current density of 0.1 $\mu\text{A}/\text{cm}^2$ for ZnO nanomaterial field emission cathode array based on graphical growth by hydrothermal method. Zhang *et al.*^[11] has reported a turn-on field of 2.4 V/ μm at a current density of 0.1 $\mu\text{A}/\text{cm}^2$ for patterned ZnO nanowires synthesized on Si substrate with

a patterned Au catalyst film. Huang *et al.*^[12] has also reported a turn-on field of 3.3 V/ μm at a current density of 0.1 $\mu\text{A}/\text{cm}^2$ for patterned ZnO nanorods grown on ITO substrate by two-step thermal evaporation method.

In this letter, we report a process technology where patterned ZnO nanowires were synthesized onto linear ITO (indium oxide doped with tin film) electrodes deposited on glass substrate (PD200) via a vapor–solid (VS) growth mode. The evaporation method is realized at a low temperature without a metallic catalyst. Furthermore, their field emission measurement results reveal that patterned ZnO nanowire arrays possess efficient field emission. It is sure that patterned ZnO nanowire arrays have a great number of potential applications for the flat panel display in the future.

2. Experimental

The schematic of fabrication process for field emission arrays (FEAs) with patterned ZnO nanowires is shown in Fig. 1. The ITO-coated glass substrate was cleaned in acetone for 30 min under ultrasonic cleaning. After rinsing the substrate by alcohol and deionized water, it was baked in a furnace at 100 °C for 30 min, as shown in Fig. 1(a). The substrate was coated with positive photoresist (RZJ-304) using spin coating and then photoresist patterns were formed by developer after UV exposure in Fig. 1(b). Etching of ITO layer on the glass substrate was carried out in an ITO etchant (mixture of hydrochloric acid and ferric trichloride). After ITO etching, the photoresist pattern was removed by acetone and cleaned by DI water. Then, ITO electrodes were obtained in Fig. 1(c). ZnO nanowires were synthesized on ITO electrodes by thermal evaporation method, as shown in Fig. 1(d). Firstly, high purity (99.99%) Zn pow-

* Project supported by the National High Technology Research and Development Program for Advanced Materials of China (No. 2008AA03A313) and the Technology Projects of Department of Education, Fujian Province, China (Nos. JA09017, JA11014).

[†] Corresponding author. Email: gtl_fzu@yahoo.com.cn

Received 27 July 2011, revised manuscript received 19 September 2011

© 2012 Chinese Institute of Electronics

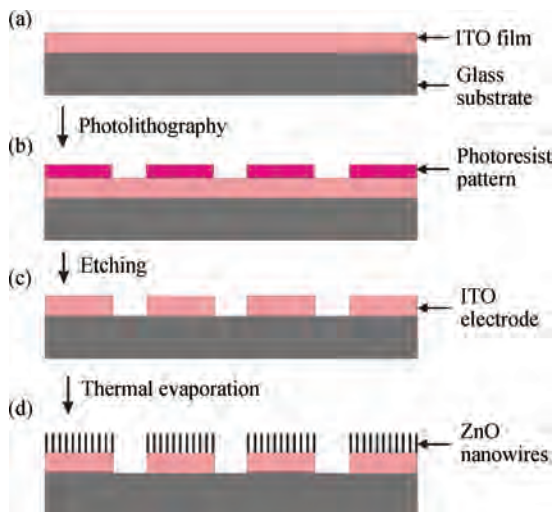


Fig. 1. Schematic of the fabrication process for field emission arrays with patterned ZnO nanowires.

der was used as the evaporation source. The synthesis process was carried out in a horizontal tube furnace, where the atmosphere, evaporation time, pressure and temperature were controlled. Secondly, the glass substrate coated with ITO electrodes was loaded on the boat. The distance between the evaporation source and the glass substrate was around 5–10 mm. The boat was placed at the centre of the furnace tube. Ar at a flow rate of 80 standard cubic centimeter per minute (scm) was used first to remove oxygen and moisture, purging the reactor for 10 min. Then the furnace was heated to 550 °C at a heating rate of 50 °C/min and kept at 550 °C for 30 min at a flow rate of 60 scm of Ar and 1 scm of O₂. Finally, patterned ZnO nanowires arrays were fabricated after cooling down the furnace naturally to room temperature under the protection of an Ar gas with flow rate of 60 scm.

The morphology of patterned ZnO nanowire arrays was characterized by scanning electron microscopy (SEM). The SEM was also employed to conduct the energy dispersive X-ray (EDX) spectroscopy and element mapping. The crystal structure and optical properties of the sample were characterized by X-ray diffraction (XRD) and photoluminescence (PL) spectroscopy, respectively. The field emission characteristics were also investigated in a vacuum chamber under a pressure of 1.5×10^{-6} Torr at room temperature.

3. Results and discussion

Figure 2(a) presents a typical image of the ITO electrodes arrays coated on the glass substrate, observed by optical microscopy. As shown in Fig. 2(a), the ITO electrodes are interdigitated and paralleled on the glass substrate. The width of electrodes is about 50 μm and the gap between the electrodes is approximately 30 μm. Figure 2(b) depicts a top-view SEM image of field emission arrays with ZnO nanowires. It is very interesting that ZnO nanowires are grown in high density over the entire surface of the linear ITO electrodes, which form the patterned ZnO nanowire arrays. Figure 2(c) shows a magnified SEM image of patterned ZnO nanowire arrays and Figure 2(d) shows a magnified SEM image of ZnO nanowires synthesized

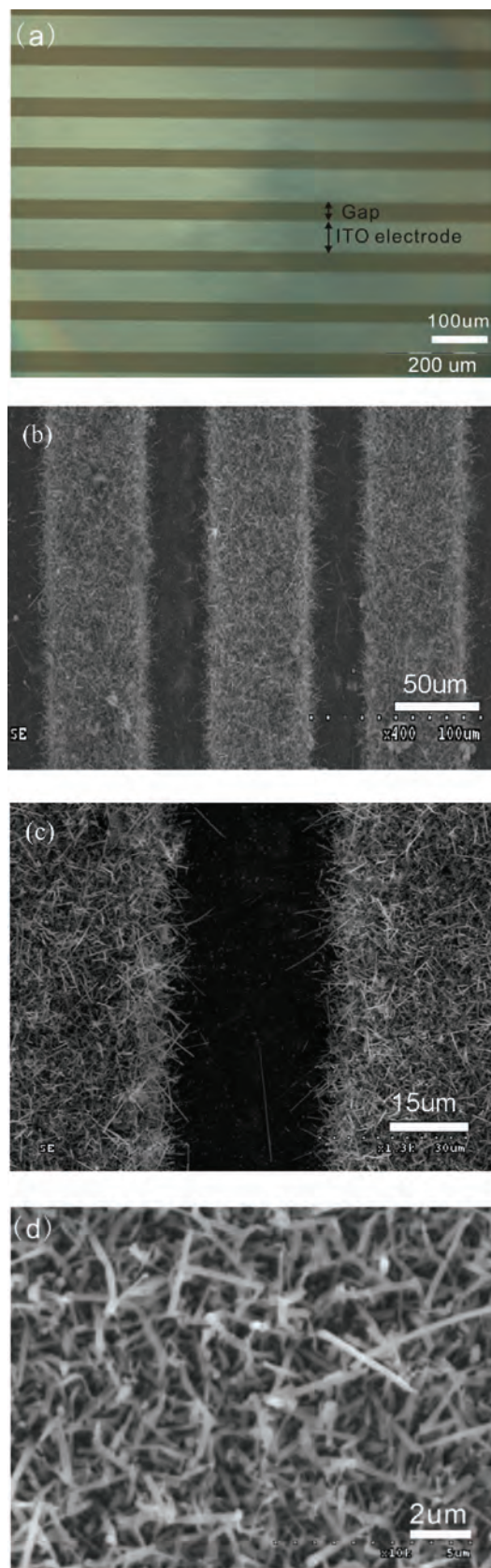


Fig. 2. (a) Optical microscope image of the ITO electrodes arrays coated on the glass substrate. (b) Top-view SEM image of field emission arrays with ZnO nanowires. (c) The magnified SEM image of the patterned ZnO nanowire arrays. (d) The magnified SEM image of ZnO nanowires on a linear ITO electrode.

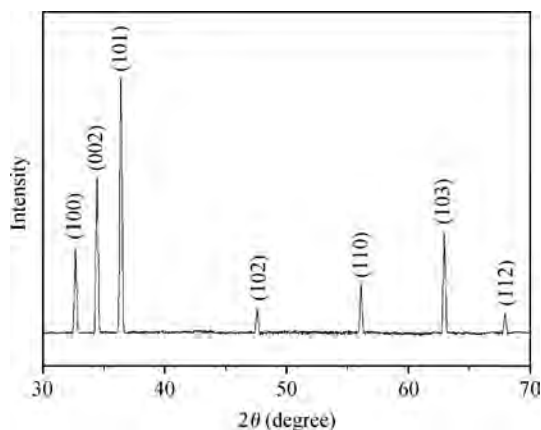


Fig. 3. XRD pattern of the synthesized sample.

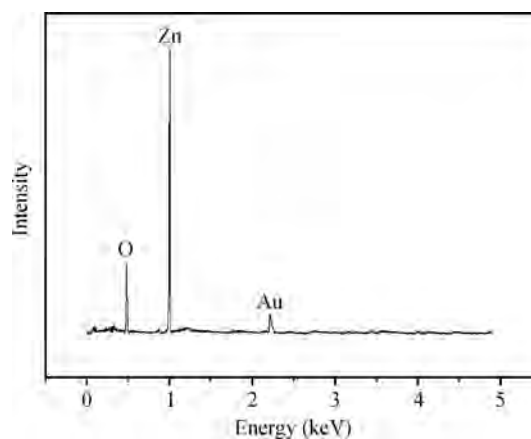


Fig. 4. EDX spectrum of the synthesized sample.

on the surface of a linear ITO electrode. The magnified SEM images clearly indicate that ZnO nanowires with the diameter of 100–200 nm and the length up to 5 μm are highly uniform and well distributed on the ITO electrodes. Further observation finds that the dense ZnO nanowires are grown upward on the linear ITO electrodes, which can make it easy to emit electrons. The growth mechanism of ZnO nanowires can be interpreted by means of the vapor-solid (VS) mechanism^[23, 24]. When the temperature was elevated to the reaction temperature, the Zn source continuously evaporated to form Zn and its suboxide (ZnO_x , $x < 1$) vapor and then transported downstream of the tube due to the flowing carrier gas. Simultaneously, the Zn and ZnO_x vapor combined with oxygen to form ZnO molecules and further grow into the nanowires on the linear ITO electrodes.

Figure 3 shows the XRD pattern of the as-synthesized ZnO nanowires. All the diffraction peaks of the XRD pattern can be readily indexed to the wurtzite structure of ZnO and the measured lattice constants are $a = 3.25 \text{ \AA}$ and $c = 5.21 \text{ \AA}$, which correspond with the data of ZnO powders recorded in the JCPDS document (Powder Diffraction File Compiled by the Joint Committee on Powder Diffraction, 1985, Card No. 80-0075). It is interesting to note that no diffraction peaks corresponding to other phases are observed, indicating the high purity of the products synthesized at reaction temperature of 550 $^\circ\text{C}$ for 30 min at an Ar flow rate of 60 sccm and O_2 flow rate of 1 sccm, respectively. In order to find the elemental composition of the sample, EDX analysis was carried out. The EDX spectrum, as shown in Fig. 4, confirms that the sample is mainly composed of Zn and O with the atom ratio of nearly 1 : 1. The Au peak may originate from the Au-sputtered sample for SEM measurement. According to the results analyzed by XRD and EDX, the products synthesized on the linear ITO electrodes should be of ZnO nanowires having wurtzite structure.

The PL was used to further investigate the optical properties of the as-synthesized ZnO nanowires. The room temperature PL spectrum measured in the spectral range of 350–600 nm is shown in Fig. 5, using a He–Cd laser at 325 nm as the excitation source. It demonstrates a strong ultraviolet emission band at approximately 383 nm, a weak blue emission band at around 470 nm and a weak green emission band at

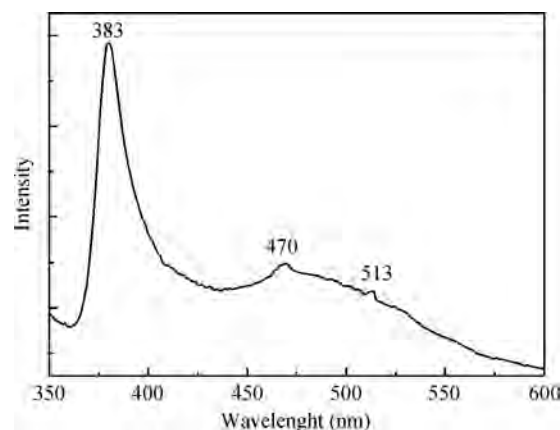


Fig. 5. PL spectrum of the ZnO nanowires measured at room temperature.

about 513 nm, respectively. The 383 nm ultraviolet emission band observed in the spectrum corresponds to the recombination of free excitons between the conduction and the valence bands; this is called the near band-edge emission^[25]. In addition to the band-edge emission, the blue emission band is observed at 470 nm, which is attributed the appearance of blue emission band originating from the oxygen vacancy^[26]. The 513 nm green emission band in the visible region, known as deep level emission, is attributed to the green transition to the singly ionized oxygen vacancy in the ZnO and the emission results from the recombination of the photo-generated hole with an electron occupying the oxygen vacancies^[27–29]. The blue-green emission can originate from oxygen vacancies and Zn interstitials^[30, 31]. The oxygen vacancies can produce shallow defect donor levels which are located below the bottom of the conduction band^[32]. Thus, it can be concluded that oxygen vacancies are the main defects causing the visible emission bands. In spite of a weak blue and green emission band, the strong ultraviolet emission band in the PL spectrum indicates that the as-synthesized ZnO nanowires at 550 $^\circ\text{C}$ for 30 min under an O_2 flow rate of 1 sccm and Ar flow rate of 60 sccm have good crystalline quality.

Field emission measurements of field emission arrays with patterned ZnO nanowires were carried out in a chamber with a vacuum of 1.5×10^{-6} Torr at room temperature. An ITO-

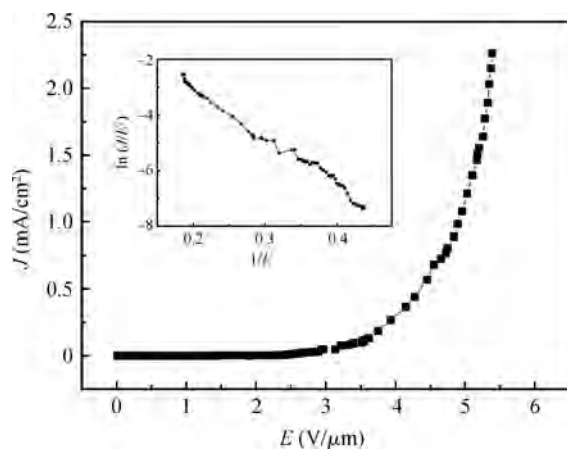


Fig. 6. Emission current density versus electric field curves of the patterned ZnO nanowire arrays. The inset is the F–N plot.

glass coated with a green phosphor film was used as an anode and the field emission arrays with patterned ZnO nanowires grown on the linear ITO electrodes as a cathode. A glass spacer of 700 μm thickness between anode and cathode was used to control the distance accurately. Figure 6 shows the dependencies of the field emission current density on the applied electric field (J – E) of ZnO nanowire arrays. Here, we define the turn-on field (E_{to}) and the threshold field (E_{thr}) as the electric fields required to produce a current density of 1 $\mu\text{A}/\text{cm}^2$ and 1 mA/cm^2 , respectively. The E_{to} and E_{thr} for patterned ZnO nanowire arrays are approximately 1.6 $\text{V}/\mu\text{m}$ and 4.92 $\text{V}/\mu\text{m}$, respectively, which is obviously lower than that of Huang's group, Zhang's group and Lin's group^[11, 12, 22]. Current density is as high as 2.26 mA/cm^2 at an applied electric field of 5.38 $\text{V}/\mu\text{m}$, indicating the efficient field emission of patterned ZnO nanowire arrays. The reasons for the low turn-on field and high emission current density are probably due to the aligned and patterned ZnO nanowires, good electrical contact with the conducting substrate where they grow and a weak field-screening effect.

The inset in Fig. 6 presents the relation between $\ln(J/E^2)$ and $1/E$. The curve shows rough linearity at high-applied fields, indicating that the emitting electrons were mainly resulted from barrier tunneling electrons extracted by the electric field and would be formulated by the Fowler–Nordheim (F–N) theory. According to the F–N law, the relationship between the emission current density (J) and the applied field strength ($E = V/d$) can be depicted as

$$J = (A\beta^2 E^2/\phi) \exp(-B\phi^{3/2}/\beta E), \quad (1)$$

where ϕ is the work function of the emitter (eV), β is the enhancement factor. A and B are constants with the value of $1.56 \times 10^{-10} \text{ A}\cdot\text{V}^{-2}\cdot\text{eV}$ and $6.83 \times 10^9 \text{ V}/(\text{eV}^{3/2}\cdot\text{m})$, respectively. The field enhancement factor β of patterned ZnO nanowire arrays can be estimated to be about 4789 from the averaged slope of the F–N plot under the assumption of a work function of 5.3 eV from ZnO emitters^[10], which is good enough for various application of field emission.

For practical application as an emitter material, the emission current density stability of patterned ZnO nanowire arrays was measured under a pressure of 1.5×10^{-6} Torr and room

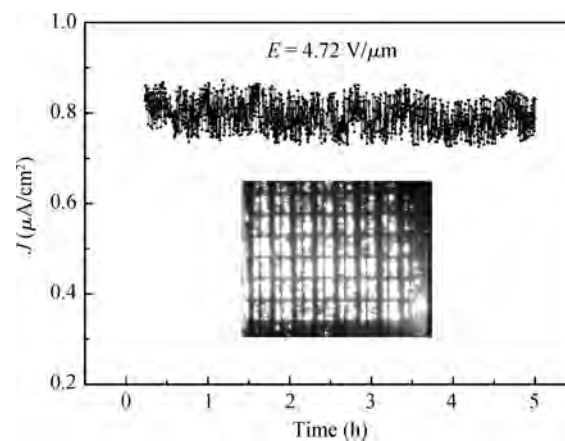


Fig. 7. Stability curve for pre-set values at 4.72 $\text{V}/\mu\text{m}$. The inset shows field emission images of field emission arrays with the patterned ZnO nanowires.

temperature at an applied electric field of around 4.72 $\text{V}/\mu\text{m}$. Figure 7 shows the result of field emission current density versus time for a period over 4.5 h. The current shows a rather high stability without detectable degradation of field emission current during the test. The current fluctuation is lower than 5%. The inset presents the electron emission images of the sample. It can be seen that the whole surface emission on the fluorescent screen is relative homogeneous. Therefore, the patterned ZnO nanowire arrays will be a promising cathode for field emission displays and vacuum electronics.

4. Conclusion

In summary, patterned ZnO nanowire arrays have been synthesized on linear ITO electrodes at low temperature of 550 $^\circ\text{C}$ without a metallic catalyst and their field emission characteristics were investigated. SEM investigations indicated that ZnO nanowires were highly uniform and well distributed on the linear ITO electrodes and formed patterned ZnO nanowire arrays. In spite of a weak blue and green emission band, the strong ultraviolet emission band in the PL spectrum demonstrated that the as-synthesized ZnO nanowires had a good crystalline quality. The field emission measurement indicated that E_{to} and E_{thr} for patterned ZnO nanowire arrays were about 1.6 $\text{V}/\mu\text{m}$ and 4.92 $\text{V}/\mu\text{m}$ with an emitter-anode gap of 700 μm , while the current density reached 2.26 mA/cm^2 at an applied field of 5.38 $\text{V}/\mu\text{m}$. A measurement of the emission stability was carried out, revealing a stable emission with a 5% fluctuation for a period over 4.5 h. The present results imply that patterned ZnO nanowire arrays are promising materials for fabricating efficient emitters in display device and vacuum electronics applications.

References

- [1] De Heer W A, Chatelain A, Ugarte D. A carbon nanotube field-emission electron source. *Science*, 1995, 270(5239): 1179
- [2] Li Z J, Ren W P, Meng A L. Morphology-dependent field emission characteristics of SiC nanowires. *Appl Phys Lett*, 2010,

- 97(26): 263117
- [3] Chueh Y L, Chou L J, Cheng S L, et al. Synthesis of taper-like Si nanowires with strong field emission. *Appl Phys Lett*, 2005, 86(13): 133112
- [4] Chen Y J, Li Q H, Liang Y X, et al. Field emission from long SnO₂ nanobelt arrays. *Appl Phys Lett*, 2004, 85(23): 5682
- [5] Bonard J M, Maier F, Stockli T, et al. Field emission properties from multiwalled carbon nanotubes. *Ultramicroscopy*, 1998, 73(1–4): 7
- [6] Dean K A, Burgin T P, Chalamala B R. Evaporation of carbon nanotubes during electron field emission. *Appl Phys Lett*, 2001, 79(12): 1873
- [7] Huang M H, Mao S, Feick H N, et al. Room-temperature ultraviolet nanowire nanolasers. *Science*, 2001, 292(5523): 1897
- [8] Liu M W, Li J H, Ma J, et al. Design and fabrication of a MEMS Lamb wave device based on ZnO thin film. *Journal of Semiconductors*, 2011, 32(4): 044006
- [9] Sun X W, Kwok H S. Optical properties of epitaxially grown zinc oxide films on sapphire by pulsed laser deposition. *J Appl Phys*, 1999, 86(1): 408
- [10] Yang X X, Lei W, Zhang X B, et al. Synthesis and efficient field emission of ZnO nanoinjectors. *Physica E*, 2009, 41(9): 1661
- [11] Zhang Y S, Yu K, Ouyang S X, et al. Patterned growth and field emission of ZnO nanowires. *Mater Lett*, 2006, 60(4): 522
- [12] Huang Y, Yu K, Zhu Z Q. Synthesis and field emission of patterned ZnO nanorods. *Curr Appl Phys*, 2007, 7(6): 702
- [13] Fu Xiaojun, Zhang Haiying, Guo Changxin, et al. Enhanced field emission of ZnO nanowires. *Journal of Semiconductors*, 2009, 30(8): 084002
- [14] Sun Y, Fuge G M, Ashfold M N R. Growth of aligned ZnO nanorod arrays by catalyst-free pulsed laser deposition methods. *Chem Phys Lett*, 2004, 396(1–3): 21
- [15] Pan Z W, Dai Z R, Wang Z L. Nanobelts of semiconducting oxides. *Science*, 2001, 291(5510): 1947
- [16] Umar A, Hahn Y B. Aligned hexagonal coaxial-shaped ZnO nanocolumns on steel alloy by thermal evaporation. *Appl Phys Lett*, 2006, 88(17): 173120
- [17] Kong X Y, Wang Z L. Spontaneous polarization-induced nano-helices, nanosprings, and nanorings of piezoelectric nanobelts. *Nano Lett*, 2003, 3(12): 1625
- [18] Wang Z L, Kong X Y, Zuo J M. Induced growth of asymmetric nanocantilever arrays on polar surfaces. *Phys Rev Lett*, 2003, 91(18): 185502
- [19] Zhang Y, Russo R E, Mao S S. Quantum efficiency of ZnO nanowire nanolasers. *Appl Phys Lett*, 2005, 87(4): 043106
- [20] Wei A, Sun X W, Xu C X, et al. Stable field emission from hydrothermally grown ZnO nanotubes. *Appl Phys Lett*, 2006, 88(21): 213102
- [21] Sheini F J, Joag D S, More M A, et al. Low temperature growth of aligned ZnO nanowires and their application as field emission cathodes. *Mater Chem Phys*, 2010, 120(8): 691
- [22] Lin Z X, Guo T L, Zhang Y A, et al. Study of the ZnO nanomaterial field emission cathode array based on graphical growth. *Acta Optica Sinica*, 2010, 30(6): 1739
- [23] Yang P, Lieber C M. Nanostructured high-temperature superconductors: creation of strong-pinning columnar defects in nanorod/superconductor composites. *J Mater Res*, 1977, 12(11): 2981
- [24] Yao B D, Chan Y F, Wang N. Formation of ZnO nanostructures by a simple way of thermal evaporation. *Appl Phys Lett*, 2002, 81(4): 757
- [25] Kong Y C, Yu D P, Zhang B, et al. Ultraviolet-emitting ZnO nanowires synthesized by a physical vapor deposition approach. *Appl Phys Lett*, 2001, 78(4): 407
- [26] Cheng W D, Wu P, Zou X Q, et al. Study on synthesis and blue emission mechanism of ZnO tetrapodlike nanostructures. *J Appl Phys*, 2006, 100(5): 054311
- [27] Umar A, Kim S H, Lee Y S, et al. Catalyst-free large-quantity synthesis of ZnO nanorods by a vapor–solid growth mechanism: structural and optical properties. *J Cryst Growth*, 2005, 282(1/2): 131
- [28] Shan F K, Kim B I, Liu G X, et al. Blueshift of near band edge emission in Mg doped ZnO thin films and aging. *J Appl Phys*, 2004, 95(9): 4772
- [29] Vanheusden K, Warren W L, Seager C H, et al. Mechanisms behind green photoluminescence in ZnO phosphor powders. *J Appl Phys*, 1996, 79(10): 7983
- [30] Wang Y G, Lau S P, Lee H W, et al. Photoluminescence study of ZnO films prepared by thermal oxidation of Zn metallic films in air. *J Appl Phys*, 2003, 94(1): 354
- [31] Lin B X, Fu Z X, Jia Y B. Green luminescent center in undoped zinc oxide films deposited on silicon substrates. *Appl Phys Lett*, 2001, 79(7): 943
- [32] Vanheusden K, Seager C H, Warren W L, et al. Correlation between photoluminescence and oxygen vacancies in ZnO phosphors. *Appl Phys Lett*, 1996, 68(3): 403